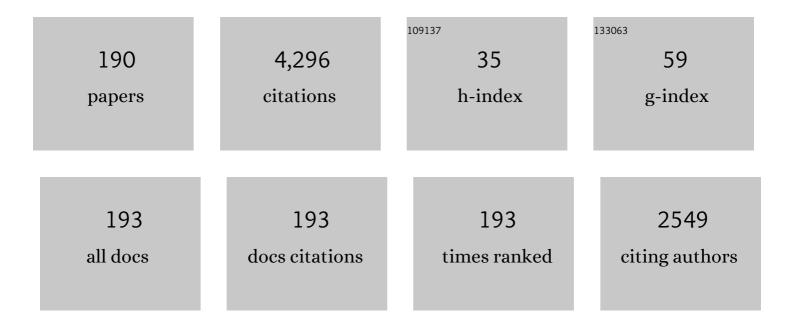
List of Publications by Year in descending order

Source: https://exaly.com/author-pdf/2544965/publications.pdf Version: 2024-02-01



TAT SOON YEO

#	Article	IF	CITATIONS
1	SAR Automatic Target Recognition Based on Multiview Deep Learning Framework. IEEE Transactions on Geoscience and Remote Sensing, 2018, 56, 2196-2210.	2.7	222
2	Imaging of a Moving Target With Rotating Parts Based on the Hough Transform. IEEE Transactions on Geoscience and Remote Sensing, 2008, 46, 291-299.	2.7	219
3	Weighted least-squares estimation of phase errors for SAR/ISAR autofocus. IEEE Transactions on Geoscience and Remote Sensing, 1999, 37, 2487-2494.	2.7	210
4	A broadband and high-gain metamaterial microstrip antenna. Applied Physics Letters, 2010, 96, .	1.5	168
5	Estimation of Three-Dimensional Motion Parameters in Interferometric ISAR Imaging. IEEE Transactions on Geoscience and Remote Sensing, 2004, 42, 292-300.	2.7	141
6	Dual-polarized slot-coupled planar antenna with wide bandwidth. IEEE Transactions on Antennas and Propagation, 2003, 51, 441-448.	3.1	124
7	A Low Profile and Low Sidelobe Wideband Slot Antenna Array Feb by an Amplitude-Tapering Waveguide Feed-Network. IEEE Transactions on Antennas and Propagation, 2015, 63, 419-423.	3.1	113
8	Noniterative quality phase-gradient autofocus (QPGA) algorithm for spotlight SAR imagery. IEEE Transactions on Geoscience and Remote Sensing, 1998, 36, 1531-1539.	2.7	107
9	A method for designing broad-band microstrip antennas in multilayered planar structures. IEEE Transactions on Antennas and Propagation, 1999, 47, 1416-1420.	3.1	85
10	Three-Dimensional ISAR Imaging Based on Antenna Array. IEEE Transactions on Geoscience and Remote Sensing, 2008, 46, 504-515.	2.7	82
11	Scattering by rotationally symmetric anisotropic spheres: Potential formulation and parametric studies. Physical Review E, 2007, 75, 026609.	0.8	78
12	A fast volume-surface integral equation solver for scattering from composite conducting-dielectric objects. IEEE Transactions on Antennas and Propagation, 2005, 53, 818-824.	3.1	75
13	Fabrication of a High-Efficiency Waveguide Antenna Array via Direct Metal Laser Sintering. IEEE Antennas and Wireless Propagation Letters, 2016, 15, 622-625.	2.4	71
14	STGRFT for Detection of Maneuvering Weak Target With Multiple Motion Models. IEEE Transactions on Signal Processing, 2019, 67, 1902-1917.	3.2	71
15	Exact solutions of electromagnetic fields in both near and far zones radiated by thin circular-loop antennas: a general representation. IEEE Transactions on Antennas and Propagation, 1997, 45, 1741-1748.	3.1	65
16	Backward waves in magnetoelectrically chiral media: Propagation, impedance, and negative refraction. Physical Review B, 2007, 75, .	1.1	61
17	A new subaperture approach to high squint SAR processing. IEEE Transactions on Geoscience and Remote Sensing, 2001, 39, 954-968.	2.7	60
18	Precorrected-FFT solution of the volume Integral equation for 3-D inhomogeneous dielectric objects. IEEE Transactions on Antennas and Propagation, 2005, 53, 313-320.	3.1	58

#	Article	IF	CITATIONS
19	Three-Dimensional Imaging of Targets Using Colocated MIMO Radar. IEEE Transactions on Geoscience and Remote Sensing, 2011, 49, 3009-3021.	2.7	57
20	A fast analysis of scattering and radiation of large microstrip antenna arrays. IEEE Transactions on Antennas and Propagation, 2003, 51, 2218-2226.	3.1	56
21	MIMO Radar 3D Imaging Based on Combined Amplitude and Total Variation Cost Function With Sequential Order One Negative Exponential Form. IEEE Transactions on Image Processing, 2014, 23, 2168-2183.	6.0	55
22	High-Resolution Bistatic ISAR Imaging Based on Two-Dimensional Compressed Sensing. IEEE Transactions on Antennas and Propagation, 2015, 63, 2098-2111.	3.1	52
23	Three-dimensional SAR imaging of a ground moving target using the InISAR technique. IEEE Transactions on Geoscience and Remote Sensing, 2004, 42, 1818-1828.	2.7	51
24	Routes to left-handed materials by magnetoelectric couplings. Physical Review B, 2007, 75, .	1.1	50
25	Radio wave propagation along mixed paths through a four-layered model of rain forest: an analytic approach. IEEE Transactions on Antennas and Propagation, 1998, 46, 1098-1111.	3.1	48
26	Microâ€Doppler feature extraction for wideband imaging radar based on complex image orthogonal matching pursuit decomposition. IET Radar, Sonar and Navigation, 2013, 7, 914-924.	0.9	45
27	Interference Cancellation for High-Frequency Surface Wave Radar. IEEE Transactions on Geoscience and Remote Sensing, 2008, 46, 1879-1891.	2.7	44
28	Wideband Bandpass Filters With SAW-Filter-Like Selectivity Using Chip SAW Resonators. IEEE Transactions on Microwave Theory and Techniques, 2014, 62, 28-36.	2.9	44
29	Bistatic ISAR Imaging Incorporating Interferometric 3-D Imaging Technique. IEEE Transactions on Geoscience and Remote Sensing, 2012, 50, 3859-3867.	2.7	43
30	A general expression of dyadic Green's functions in radially multilayered chiral media. IEEE Transactions on Antennas and Propagation, 1995, 43, 232-238.	3.1	41
31	Time-varying step-transform algorithm for high squint SAR imaging. IEEE Transactions on Geoscience and Remote Sensing, 1999, 37, 2668-2677.	2.7	39
32	Motion Parameter Estimation in the SAR System With Low PRF Sampling. IEEE Geoscience and Remote Sensing Letters, 2010, 7, 450-454.	1.4	39
33	High-Resolution Bistatic ISAR Image Formation for High-Speed and Complex-Motion Targets. IEEE Journal of Selected Topics in Applied Earth Observations and Remote Sensing, 2015, 8, 3520-3531.	2.3	39
34	Wide-band microstrip antenna with an H-shaped coupling aperture. IEEE Transactions on Vehicular Technology, 2002, 51, 17-27.	3.9	38
35	Microwave attenuation by realistically distorted raindrops: Part I. Theory. IEEE Transactions on Antennas and Propagation, 1995, 43, 811-822.	3.1	37
36	Fast analysis of scattering by arbitrarily shaped three-dimensional objects using the precorrected-FFT method. Microwave and Optical Technology Letters, 2002, 34, 438-442.	0.9	37

#	Article	IF	CITATIONS
37	Application of DCIM to MPIE-MoM analysis of 3D PEC objects in multilayered media. IEEE Transactions on Antennas and Propagation, 2002, 50, 157-162.	3.1	36
38	A novel lacunarity estimation method applied to SAR image segmentation. IEEE Transactions on Geoscience and Remote Sensing, 2002, 40, 2687-2691.	2.7	36
39	Analysis of Probe-Fed Conformal Microstrip Antennas on Finite Grounded Substrate. IEEE Transactions on Antennas and Propagation, 2006, 54, 554-563.	3.1	35
40	Transient interference excision in over-the-horizon radar using adaptive time-frequency analysis. IEEE Transactions on Geoscience and Remote Sensing, 2005, 43, 722-735.	2.7	34
41	Sparse Array 3-D ISAR Imaging Based on Maximum Likelihood Estimation and CLEAN Technique. IEEE Transactions on Image Processing, 2010, 19, 2127-2142.	6.0	34
42	Three-Dimensional Imaging Using Colocated MIMO Radar and ISAR Technique. IEEE Transactions on Geoscience and Remote Sensing, 2012, 50, 3189-3201.	2.7	34
43	Computational Efficient Refocusing and Estimation Method for Radar Moving Target With Unknown Time Information. IEEE Transactions on Computational Imaging, 2020, 6, 544-557.	2.6	34
44	Analysis of radiowave propagation in a four-layered anisotropic forest environment. IEEE Transactions on Geoscience and Remote Sensing, 1999, 37, 1967-1979.	2.7	32
45	A Fast Combined Field Volume Integral Equation Solution to EM Scattering by 3-D Dielectric Objects of Arbitrary Permittivity and Permeability. IEEE Transactions on Antennas and Propagation, 2006, 54, 961-969.	3.1	32
46	Receiver Design for MIMO Radar Range Sidelobes Suppression. IEEE Transactions on Signal Processing, 2010, 58, 5469-5474.	3.2	30
47	Wideband Dual-Polarized and Dual-Monopulse Compact Array for SAR System Integration Applications. IEEE Geoscience and Remote Sensing Letters, 2016, 13, 1203-1207.	1.4	30
48	Waveguide-Stripline Series–Corporate Hybrid Feed Technique for Dual-Polarized Antenna Array Applications. IEEE Transactions on Components, Packaging and Manufacturing Technology, 2017, 7, 81-87.	1.4	28
49	Refocusing and Zoom-In Polar Format Algorithm for Curvilinear Spotlight SAR Imaging on Arbitrary Region of Interest. IEEE Transactions on Geoscience and Remote Sensing, 2019, 57, 7995-8010.	2.7	28
50	FAST ANALYSIS OF ELECTROMAGNETIC TRANSMISSION THROUGH ARBITRARILY SHAPED AIRBORNE RADOMES USING PRECORRECTED-FFT METHOD. Progress in Electromagnetics Research, 2005, 54, 37-59.	1.6	26
51	INTERFEROMETRIC ISAR IMAGING ON SQUINT MODEL. Progress in Electromagnetics Research Letters, 2008, 2, 125-133.	0.4	26
52	Multi-Frame Integration Method for Radar Detection of Weak Moving Target. IEEE Transactions on Vehicular Technology, 2021, 70, 3609-3624.	3.9	26
53	Analysis of metallic waveguides of a large class of cross sections using polynomial approximation and superquadric functions. IEEE Transactions on Microwave Theory and Techniques, 2001, 49, 1136-1139.	2.9	25
54	Unambiguous Reconstruction and High-Resolution Imaging for Multiple-Channel SAR and Airborne Experiment Results. IEEE Geoscience and Remote Sensing Letters, 2009, 6, 102-106.	1.4	25

#	Article	IF	CITATIONS
55	Radio Frequency Interference Suppression for SAR via Block Sparse Bayesian Learning. IEEE Journal of Selected Topics in Applied Earth Observations and Remote Sensing, 2018, 11, 4835-4847.	2.3	25
56	Spheroidal vector wave eigenfunction expansion of dyadic Green's functions for a dielectric spheroid. IEEE Transactions on Antennas and Propagation, 2001, 49, 645-659.	3.1	23
57	A fast analysis of electromagnetic scattering by arbitrarily shaped homogeneous dielectric objects. Microwave and Optical Technology Letters, 2003, 38, 30-35.	0.9	23
58	ISAR imaging in strong ground clutter using a new stepped-frequency signal format. IEEE Transactions on Geoscience and Remote Sensing, 2003, 41, 948-952.	2.7	23
59	Three-Dimensional ISAR Imaging Using a Two-Dimensional Sparse Antenna Array. IEEE Geoscience and Remote Sensing Letters, 2008, 5, 378-382.	1.4	23
60	Generalized Omega-K Algorithm for Geosynchronous SAR Image Formation. IEEE Geoscience and Remote Sensing Letters, 2015, 12, 2286-2290.	1.4	23
61	Bistatic ISAR distortion and defocusing analysis. IEEE Transactions on Aerospace and Electronic Systems, 2016, 52, 1168-1182.	2.6	23
62	Wave Mode and Path Characteristics in a Four-Layered Anisotropic Forest Environment. IEEE Transactions on Antennas and Propagation, 2004, 52, 2445-2455.	3.1	22
63	Propagation property analysis of metamaterial constructed by conductive SRRs and wires using the MGS-based algorithm. IEEE Transactions on Microwave Theory and Techniques, 2005, 53, 1469-1476.	2.9	22
64	Input impedance of a probe-excited semi-infinite rectangular waveguide with arbitrary multilayered loads. I. Dyadic Green's functions. IEEE Transactions on Microwave Theory and Techniques, 1995, 43, 1559-1566.	2.9	21
65	Radiation of an aperture antenna covered by a spherical-shell chiral radome and fed by a circular waveguide. IEEE Transactions on Antennas and Propagation, 1998, 46, 664-671.	3.1	19
66	Small dual-frequency microstrip antennas. IEEE Transactions on Vehicular Technology, 2002, 51, 28-36.	3.9	19
67	Design of a symmetric rectangular waveguide T-junction with in-phase and unequal power split characteristics. , 2013, , .		19
68	Three-dimensional visible-light capsule enclosing perfect supersized darkness via antiresolution. Laser and Photonics Reviews, 2014, 8, 743-749.	4.4	19
69	Fast Marginalized Sparse Bayesian Learning for 3-D Interferometric ISAR Image Formation Via Super-Resolution ISAR Imaging. IEEE Journal of Selected Topics in Applied Earth Observations and Remote Sensing, 2015, 8, 4942-4951.	2.3	19
70	Multiview Synthetic Aperture Radar Automatic Target Recognition Optimization: Modeling and Implementation. IEEE Transactions on Geoscience and Remote Sensing, 2018, 56, 6425-6439.	2.7	19
71	Cylindrical Vector Eigenfunction Expansion of Green Dyadics for Multilayered Anisotropic Media and Its Application to Four-Layered Forest. IEEE Transactions on Antennas and Propagation, 2004, 52, 466-477.	3.1	18
72	Target imaging based on â"" <sub>1</sub> â"" <sub>0</sub> norms homotopy sparse signal recovery and distributed MIMO antennas. IEEE Transactions on Aerospace and Electronic Systems, 2015, 51, 3399-3414.	2.6	18

#	Article	IF	CITATIONS
73	Electromagnetic radiation from a prolate spheroidal antenna enclosed in a confocal spheroidal radome. IEEE Transactions on Antennas and Propagation, 2002, 50, 1525-1533.	3.1	17
74	Enhanced LRR-Based RFI Suppression for SAR Imaging Using the Common Sparsity of Range Profiles for Accurate Signal Recovery. IEEE Transactions on Geoscience and Remote Sensing, 2021, 59, 1302-1318.	2.7	17
75	Rectangular modes and dyadic Green's functions in a rectangular chirowaveguide. I. Theory. IEEE Transactions on Microwave Theory and Techniques, 1999, 47, 67-73.	2.9	16
76	Adaptive Clutter Suppression in Randomized Stepped-Frequency Radar. IEEE Transactions on Aerospace and Electronic Systems, 2021, 57, 1317-1333.	2.6	16
77	An efficient calculational approach to evaluation of microwave specific attenuation. IEEE Transactions on Antennas and Propagation, 2000, 48, 1220-1229.	3.1	15
78	Cutoff wavenumbers in truncated waveguides. IEEE Microwave and Wireless Components Letters, 2001, 11, 214-216.	2.0	14
79	A Comparative Study of Radio Wave Propagation Over the Earth Due to a Vertical Electric Dipole. IEEE Transactions on Antennas and Propagation, 2007, 55, 2723-2732.	3.1	14
80	Three-dimensional aircraft isar imaging based on shipborne radar. IEEE Transactions on Aerospace and Electronic Systems, 2016, 52, 2504-2518.	2.6	14
81	Focusing of Tandem Bistatic-Configuration Data With Range Migration Algorithm. IEEE Geoscience and Remote Sensing Letters, 2011, 8, 88-92.	1.4	13
82	A Wideband Bandpass Filter With Frequency Selectivity Controlled by SAW Resonators. IEEE Transactions on Components, Packaging and Manufacturing Technology, 2016, 6, 897-905.	1.4	13
83	Imaging for Small UAV-Borne FMCW SAR. Sensors, 2019, 19, 87.	2.1	13
84	Analysis of hollow conducting waveguides using superquadric functions-A unified representation. IEEE Transactions on Microwave Theory and Techniques, 2000, 48, 876-880.	2.9	12
85	Multiple penetration of a TE/sub z/-polarized plane wave into multilayered cylindrical cavity-backed apertures. IEEE Transactions on Electromagnetic Compatibility, 2000, 42, 330-338.	1.4	11
86	The near-zone field characteristics of an E-polarization plane wave penetrating through cylindrical multiple apertures (non) coated with lossy and lossless media. IEEE Transactions on Electromagnetic Compatibility, 2002, 44, 329-337.	1.4	11
87	Eigenfunctional representation of dyadic Green's functions in multilayered gyrotropic chiral media. Journal of Physics A: Mathematical and Theoretical, 2007, 40, 5751-5766.	0.7	11
88	Two types of waveguide comparator for wideband monopulse antenna array application. , 2015, , .		11
89	An Efficient Method for Single-Channel SAR Target Reconstruction Under Severe Deceptive Jamming. IEEE Geoscience and Remote Sensing Letters, 2020, 17, 237-241.	1.4	11
90	Electromagnetic dyadic Green's functions for multilayered spheroidal structures. I: formulation. IEEE Transactions on Microwave Theory and Techniques, 2001, 49, 532-541.	2.9	10

#	Article	IF	CITATIONS
91	Circular cylindrical waveguide filled with uniaxial anisotropic media electromagnetic fields and dyadic Green's functions. IEEE Transactions on Microwave Theory and Techniques, 2001, 49, 1361-1364.	2.9	10
92	Range Sidelobe Suppression for Randomized Stepped-Frequency Chirp Radar. IEEE Transactions on Aerospace and Electronic Systems, 2021, 57, 3874-3885.	2.6	10
93	MIMO Waveform Design for Dual Functions of Radar and Communication With Space-Time Coding. IEEE Journal on Selected Areas in Communications, 2022, 40, 1906-1917.	9.7	10
94	An efficient TCS formula for rainfall microwave attenuation: T-matrix approach and 3-D fitting for oblate spheroidal raindrops. IEEE Transactions on Antennas and Propagation, 1998, 46, 1176-1181.	3.1	9
95	Stacked Phased Array Coils for Increasing the Signal-to-Noise Ratio in Magnetic Resonance Imaging. IEEE Transactions on Biomedical Circuits and Systems, 2013, 7, 24-30.	2.7	9
96	Central DOA Estimation of Incoherently Distributed Noncircular Sources with Cross-Correlation Matrix. Circuits, Systems, and Signal Processing, 2015, 34, 3697-3707.	1.2	9
97	Defocusing and distortion elimination for shipborne bistatic ISAR. Remote Sensing Letters, 2016, 7, 523-532.	0.6	9
98	An Over-Complete Dictionary Design Based on GSR for SAR Image Despeckling. IEEE Geoscience and Remote Sensing Letters, 2017, 14, 2230-2234.	1.4	9
99	Co-Located MIMO Radar Target Detection in Cluttered and Noisy Environment Based on 2D Block Sparse Recovery. IEEE Transactions on Signal Processing, 2021, 69, 3431-3445.	3.2	9
100	Improved Signal-to-Noise Ratio Performance in Magnetic Resonance Imaging by Using a Multilayered Surface Coil Array—A Simulation Study. IEEE Journal of Biomedical and Health Informatics, 2013, 17, 756-762.	3.9	8
101	Focusing of geosynchronous SAR with nonlinear chirp scaling algorithm. Electronics Letters, 2015, 51, 1195-1197.	0.5	8
102	MIMO waveform design combined with constellation mapping for the integrated system of radar and communication. Signal Processing, 2020, 170, 107443.	2.1	8
103	Compressive Sensing SAR Imaging Algorithm for LFMCW Systems. IEEE Transactions on Geoscience and Remote Sensing, 2021, 59, 8486-8500.	2.7	8
104	Efficient analysis of electromagnetic scattering and radiation from patches on finite, arbitrarily curved, grounded substrates. Radio Science, 2004, 39, n/a-n/a.	0.8	7
105	Fast median filtering algorithm based on FPGA. , 2010, , .		7
106	Wideband bandpass filters with high passband selectivity using SAW-like resonators. , 2013, , .		7
107	Design of a wideband and low-profile monopulse array fabricated by 3-d metal printing technique. , 2015, , .		7
108	Robust GMTI Scheme for Highly Squinted Hypersonic Vehicle-Borne Multichannel SAR in Dive Mode. Remote Sensing, 2021, 13, 4431.	1.8	7

#	Article	IF	CITATIONS
109	A novel technique for the processing of short-dwell spotlight SAR data. IEEE Transactions on Geoscience and Remote Sensing, 2003, 41, 953-963.	2.7	6
110	Increasing the Signal-to-Noise Ratio by Using Vertically Stacked Phased Array Coils for Low-Field Magnetic Resonance Imaging. IEEE Transactions on Information Technology in Biomedicine, 2012, 16, 1150-1156.	3.6	6
111	Physically symmetric wideband waveguide <scp>T</scp> â€junction with equalâ€phase and unequalâ€power division. Microwave and Optical Technology Letters, 2015, 57, 1216-1219.	0.9	6
112	Multiple input multiple output radar imaging based on multidimensional linear equations and sparse signal recovery. IET Radar, Sonar and Navigation, 2018, 12, 3-10.	0.9	6
113	Input impedance of a probe-excited semi-infinite rectangular waveguide with arbitrary multilayered loads: part II-a full-wave analysis. IEEE Transactions on Microwave Theory and Techniques, 1997, 45, 321-329.	2.9	5
114	Accurate Analysis of Meanderline Polarizers With Finite Thicknesses Using Mode Matching. IEEE Transactions on Antennas and Propagation, 2008, 56, 3580-3585.	3.1	5
115	Application of 3-D metal-direct-printing technique for waveguide antenna fabrication. , 2015, , .		5
116	Novel sparse apertures ISAR imaging algorithm via the TLSâ€ESPRIT technique. IET Radar, Sonar and Navigation, 2020, 14, 852-859.	0.9	5
117	Radio Wave Propagation along Earth-Space Paths in the Presence of a Multilayered Anisotropic Forest. Electromagnetics, 2002, 22, 235-260.	0.3	4
118	Convergence acceleration for calculating radiated fields by a vertical electric dipole in the presence of a large sphere. , 0, , .		4
119	On the Integral Identities Consisting of Two Spherical Bessel Functions. IEEE Transactions on Antennas and Propagation, 2007, 55, 240-244.	3.1	4
120	ASED-AIM ANALYSIS OF SCATTERING BY LARGE-SCALE FINITE PERIODIC ARRAYS. Progress in Electromagnetics Research B, 2009, 18, 381-399.	0.7	4
121	Zero Correlation Zone Codes and Extended Zero Correlation Zone Codes for MIMO radar signal separation. , 2010, , .		4
122	Power distributions in breast and heart during microwave breast cancer treatment. , 2010, , .		4
123	A phased coil array for efficient wireless power transmission. , 2012, , .		4
124	Application of X-ray scanning to diagnose internal details of waveguide antenna fabricated by 3-D metal-direct-printing technique. , 2015, , .		4
125	Precision Downward-Looking 3D Synthetic Aperture Radar Imaging with Sparse Linear Array and Platform Motion Parameters Estimation. Remote Sensing, 2018, 10, 1957.	1.8	4
126	Rectangular modes and dyadic Green's functions in a rectangular chirowaveguide. II. Results. IEEE Transactions on Microwave Theory and Techniques, 1999, 47, 74-81.	2.9	3

#	Article	IF	CITATIONS
127	QZ Factorization for generalized eigenvalues applied to waveguide analysis. Microwave and Optical Technology Letters, 2001, 28, 361-364.	0.9	3
128	Increase the signal-to-noise ratio of magnetic resonance imaging by a vertical coil array. , 2012, , .		3
129	Sparsity-Inducing Super-Resolution Passive Radar Imaging with Illuminators of Opportunity. Remote Sensing, 2016, 8, 929.	1.8	3
130	Curvilinear Video-SAR Persistent Imaging with Distortion Correction Based on Nufft-3. , 2019, , .		3
131	Accurate SAR Image Recovery From RFI Contaminated Raw Data by Using Image Domain Mixed Regularizations. IEEE Transactions on Geoscience and Remote Sensing, 2022, 60, 1-13.	2.7	3
132	A Novel Algorithm for Hypersonic SAR Imaging With Large Squint Angle and Dive Trajectory. IEEE Geoscience and Remote Sensing Letters, 2022, 19, 1-5.	1.4	3
133	Three-dimensional interferometric imaging and micromotion feature extraction of spinning space debris in low-resolution radar. Journal of Applied Remote Sensing, 2018, 12, 1.	0.6	3
134	Modal analysis of waveguides and efficient CAD of waveguide junctions using a unified method. , 0, , .		2
135	Cylindrical vector wave function representation of Green's dyadics for uniaxial bianisotropic media. , 0, , .		2
136	Cylindrical vector wave function representation of Green's dyadics for uniaxial bianisotropic media. Radio Science, 2001, 36, 517-523.	0.8	2
137	Symbolic derivation and numeric computation of dyadic Green's functions using Mathematica. IEEE Antennas and Propagation Magazine, 2001, 43, 108-118.	1.2	2
138	Indirect modelling of the scattering from two-dimensional composite uniaxial bianisotropic cylinders of arbitrary cross-sections. International Journal of Numerical Modelling: Electronic Networks, Devices and Fields, 2001, 14, 237-256.	1.2	2
139	Lightning Interference Cancellation in High-Frequency Surface Wave Radar. , 2006, , .		2
140	ISAR imaging of targets with moving parts using micro-doppler detection on the range profile image. , 2007, , .		2
141	Threshold-based Incomplete LU Factorization Preconditioner for Adaptive Integral Method. , 2007, , .		2
142	Micro-motion feature extraction of target in inverse synthetic aperture radar imaging with sparse aperture. Journal of Electromagnetic Waves and Applications, 2013, 27, 1841-1849.	1.0	2
143	Micromotion feature extraction of radar target using tracking pulses with adaptive pulse repetition frequency adjustment. Journal of Applied Remote Sensing, 2014, 8, 083569.	0.6	2
144	High-efficiency waveguide antenna with 3-D metal-direct-printing technique. , 2015, , .		2

TAT SOON YEO

#	Article	IF	CITATIONS
145	Accurate slant range model and focusing method in geosynchronous SAR. , 2015, , .		2
146	Adaptive Resource Allocation Scheme for Micromotion Feature Extraction Based on Track-Before-Detect. Journal of Sensors, 2018, 2018, 1-13.	0.6	2
147	Cutoff frequencies of an asymmetrically loaded cylindrical waveguide. IEEE Transactions on Microwave Theory and Techniques, 1998, 46, 1331-1334.	2.9	1
148	An improved step transform algorithm for high squint angle SAR imaging. , 1998, , .		1
149	Dyadic Green's functions in multilayered stratified gyroelectric chiral media. , 2000, , .		1
150	Analysis of antenna arrays with finite frequency selective surfaces. , 2006, , .		1
151	Computational study of significant semi-infinite integrals in electromagnetic and atomic interactions. , 2006, , .		1
152	Range and cross range joint processing of MIMO radar using DS-CDMA signal. , 2008, , .		1
153	An accurate and robust approach for evaluating VIE impedance matrix elements using SWG basis functions. , 2008, , .		1
154	Implementation of parallel GMRES(m) FFT method for solving large scale electromagnetic problems. Microwave and Optical Technology Letters, 2009, 51, 2084-2087.	0.9	1
155	A K <inf>a</inf> -band lumped element dual-behavior resonator (DBR) filter in standard 0.13-μm CMOS technology. , 2013, , .		1
156	A filter with reconfigurable band edges using dual-behavior resonators. , 2014, , .		1
157	Doppler parameters estimation for bistatic forward-looking SAR via ACFT. , 2015, , .		1
158	On compensation of Migration Through Resolution Cells in ISAR imaging. , 2015, , .		1
159	Matrix Ill-Condition Analysis in Spectrum Recovery of DPCA HRWS SAR Imaging. IEEE Geoscience and Remote Sensing Letters, 2019, 16, 55-59.	1.4	1
160	High-Resolution Wide-Swath SIMO and MIMO SAR Imaging Using Short-Term Shift Orthogonal Code. IEEE Geoscience and Remote Sensing Letters, 2020, 17, 92-96.	1.4	1
161	Bi-static high resolution imaging for ship targets with sparse apertures and its application in InISAR. Remote Sensing Letters, 2020, 11, 545-554.	0.6	1
162	An optimal method for phase error estimation in SAR imagery. , 1998, , .		0

#	Article	IF	CITATIONS
163	The interaction of a Gaussian beam wave with an array of slit-coupled cylindrical-impedance screens. Microwave and Optical Technology Letters, 2000, 27, 248-252.	0.9	Ο
164	Discrete analysis of a 3-dimensional airborne radome of superspheroidal shapes. , 2000, , .		0
165	Electromagnetic scattering by a multilayer gyrotropic bianisotropic cylinder. , 0, , .		о
166	Correct characterization of guided electromagnetic waves in chirowaveguides of arbitrary cross sections. Radio Science, 2001, 36, 525-531.	0.8	0
167	Dominant lateral waves of radio communication in layered anisotropic forest environment. , 0, , .		0
168	The application of the generalized conjugate residual algorithm to accelerate the fast multipole method. , 0, , .		0
169	Efficient numerical modeling of large-scale microstrip structures. , 0, , .		0
170	Precorrected-FFT solution of the volume integral equations for inhomogeneous dielectric bodies. , 0, , .		0
171	Representations of green's dyadics in multilayered general faraday chiral media. , 0, , .		0
172	Field representations in general gyrotropic media in spherical coordinates. , 0, , .		0
173	An efficient technique for optimization of the concentric array radial line slot antenna (CA-RLSA). , 2005, , .		0
174	Efficient Analysis of Probe-fed Microstrip Antennas on Arbitrarily Shaped, Finite Ground Plane and Substrate. , 0, , .		0
175	A Novel Method for Computing Admittances of Radial Line Slot Antennas. , 0, , .		Ο
176	Parallel FFT Based Fast Algorithms for Solving Large Scale Electromagnetic Problems. , 2006, , .		0
177	ISAR Imaging Enhancement Using Vernier Ranging Method. , 2006, , .		Ο
178	ISAR imaging of helicopter. , 2007, , .		0
179	Wideband and low loss metamaterials for microwave and RF applications: Fast algorithm and antenna design. , 2008, , .		Ο
180	Two dimensional imaging of extended targets by MIMO radar using hopped frequency signal. , 2008, , .		0

TAT SOON YEO

#	Article	IF	CITATIONS
181	Realization of efficient wireless power transmission by a vertical coil array. , 2012, , .		0
182	Design of phased array coils for increasing the signal-to-noise ratio of magnetic resonance imaging. , 2012, , .		0
183	Applying Taylor's distribution to 2×2 uniformly-fed sub-arrays. , 2013, , .		0
184	A 2×2 waveguide-fed antenna array with more than 25% bandwidth in the Ku-band. , 2015, , .		0
185	Geosynchronous synthetic aperture radar data focusing based on extended keystone transform. Journal of Applied Remote Sensing, 2015, 9, 095042.	0.6	Ο
186	Parameter estimation of incoherently distributed source based on block sparse Bayesian learning. , 2015, , .		0
187	Analysis for integration time and resolution in geosynchronous SAR. , 2016, , .		0
188	Signal Processing for Small-squinted Multi-rotor UAV-borne FMCW SAR. , 2019, , .		0
189	Radar Signal Processing. , 0, , .		0
190	Coherent processing for randomized steppedâ€frequency radar in multiâ€target scenario. IET Radar, Sonar and Navigation, 0, , .	0.9	0